P1.3 MONITORING THE OCEAN ACOUSTICALLY: A REVIEW AND STRATEGY FOR THE FUTURE

Bruce M. Howe* and Brian D. Dushaw
Applied Physics Laboratory, University of Washington, Seattle, Washington
and
Walter H. Munk and Peter F. Worcester
Scripps Institution of Oceanography, University of California at San Diego, La Jolla, California

ABSTRACT

Since it was first proposed in the late 1970s (Munk and Wunsch 1979, 1982), ocean acoustic tomography has evolved into a remote sensing technique employed in a wide variety of physical settings. In the context of long-term oceanic climate change, acoustic tomography provides integrals through the mesoscale and other high-wavenumber noise over long distances. In addition, tomographic measurements can be made without risk of calibration drift; these measurements have the accuracy and precision required for large-scale ocean climate observation. The trans-basin acoustic measurements offer a signal-to-noise capability for observing ocean climate variability that is not readily attainable by an ensemble of point measurements.

On a regional scale, tomography has been employed for observing active convection, for measuring changes in integrated heat content, for observing the mesoscale with high resolution, for measuring barotropic currents in a unique way, and for directly observing oceanic relative vorticity. The remote sensing capability has proven effective for measurements under ice in the Arctic (in particular the recent well-documented temperature increase in the Atlantic layer) and in regions such as the Strait of Gibraltar, where conventional *in situ* methods may fail.

As the oceanographic community moves into an era of global-scale observations, the role for these acoustic techniques will be (1) to exploit the unique remote sensing capabilities for regional programs otherwise difficult to carry out, (2) to be a component of process-oriented experiments in regions where integral heat content or current data are desired, and (3) to move toward deployment on basin scales as the acoustic technology becomes more robust and simplified.

1. FUNDAMENTALS

Sound travels faster in warm water than in cold water. By measuring the travel time of sound over a known path, the sound speed and thus temperature can be determined. Sound also travels faster with a current than against. By measuring the reciprocal travel times in each direction along a path, the absolute water velocity can be determined. In ocean acoustic tomography, data from a multitude of such paths crossing at many different angles are used to reconstruct the sound speed (temperature) and velocity fields (Fig. 1).

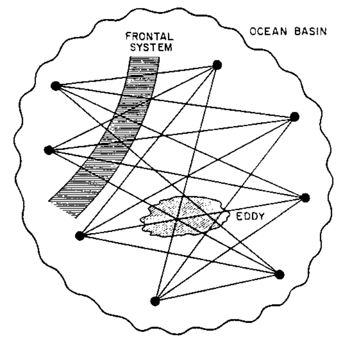

Fig 1. Acoustic paths through eddies and fronts.

Each acoustic travel time represents the path integral of the sound speed (temperature) and water velocity. As the sound travels along a ray path, it inherently averages these properties of the ocean, heavily filtering along-path horizontal scales shorter than the path length. Over a 1000-km range, a depth-averaged temperature change of 10 m°C is easily measured as a 20-ms travel time change. (Munk, Worcester, and Wunsch, 1995)

In temperate oceans, a sound speed minimum occurs at about 1 km depth. This deep ocean sound channel, or waveguide, traps acoustic energy in the water column so that it can propagate great distances without interacting with the ocean bottom. The sound channel also causes multiple acoustic paths, called eigenrays, between an acoustic source and a receiver. The different turning depths of the paths cause the acoustic pulses along those paths to have different travel times. An acoustic receiver detects the arrival of multiple pulses, and each pulse can be identified with a predicted ray path.

1.1 *AMODE-MST–Mesoscale Mapping Over a Large Area*

One of the original goals of tomography was to observe synoptically the mesoscale variability of the ocean. The Acoustic Mid-Ocean Dynamics Experiment/Moving Ship Tomography (AMODE-MST) obtained high resolution, nearly synoptic 3-D maps of the ocean over a large area, (Fig. 2; Cornuelle et al., 1989; The AMODE Group, 1994).

A ship with an acoustic receiving array steamed around the 1000-km diameter circle, stopping every 3 hours (~ 25 km) to receive signals from six moored sources. The acous-

Corresponding author address: Bruce M. Howe, Applied Physics Laboratory, 1013 NE 40th Street, Seattle, WA, 98105; e-mail: howe@apl.washington.edu.

tic travel time data were inverted to produce the field (Fig. 2, top left). Two independent estimates of the sound speed, one based on the acoustic data, and one based on AXBT data, agree within the uncertainties of each method.

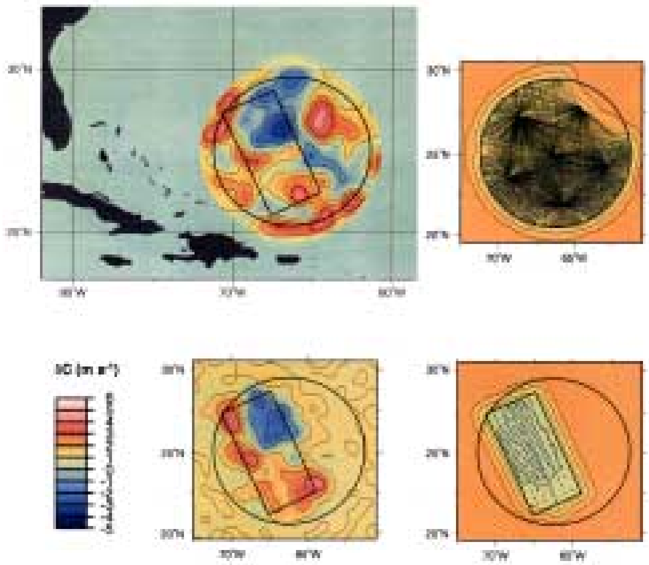

Fig. 2. (Top left) Sound speed perturbation at 700 m depth as measured during the MST experiment (July 15–30, 1991; 1 $ms^{-1} \approx 0.25°C$). (Bottom left) This map was obtained using only air-expendable bathythermograph (AXBT) data at 700 m (July 18–22). The panels at right show the line-integral or point sampling that was used to obtain the maps on the left, with estimated errors.

2. PROCESS EXPERIMENTS

2.1 *Heat Content, Velocity, and Vorticity in the North Pacific*

The 1987 reciprocal acoustic tomography experiment (RTE87) obtained unique measurements of gyre-scale temperature and currents (Fig. 3; Dushaw et al., 1993, 1994). The vorticity is calculated by integrating the currents around the experiment triangle. The calculation of vorticity cancels much of the variability of the currents. The acoustic estimates of the time varying heat content are very smooth with small uncertainty.

2.2 *Control Points–Strait of Gibraltar*

The Strait of Gibraltar is a control point for the entire Mediterranean Sea. Mass, heat, and salt are exchanged with the Atlantic Ocean. The intense and highly turbulent flow makes tomography an attractive measurement approach because it provides the necessary integration to estimate net transports. A pilot experiment has been conducted (Fig. 4; Send et al., 2000). The agreement between along-strait current averaged along a deep-turning acoustic ray and independent measurements is very good. A permanent system for sustained observations is planned.

2.3 *Deep Convection–Greenland and Labrador Seas*

Oceanic convection connects the surface ocean to the deep ocean with important consequences for the global thermohaline circulation and climate. Deep convection occurs in only a few locations in the world, and is difficult to observe. Acoustic arrays provide both the spatial coverage and temporal resolution necessary to observe deep-water formation. An experiment in the Greenland Sea ob-

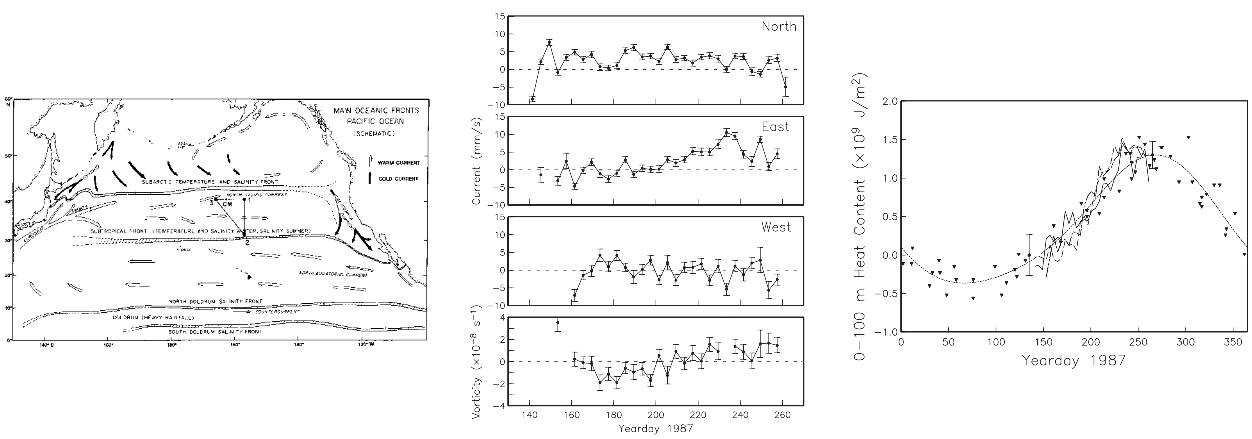

Fig 3. (Left) Geometry of the RTE87 gyre-scale reciprocal acoustic tomography experiment, with acoustic transceivers at locations 1, 2, and 3. The ranges of the acoustic paths were 750, 1000, and 1250 km. (Center) The low frequency (daily averaged) barotropic currents for each leg and the areal averaged relative vorticity. (Right) Comparisons of the acoustically determined heat content change in the top 100 m (curves between day 150 and 260) with other estimates (triangles from XBTs, points with error bars from CTDs).

served the formation of a deep convective chimney (Fig. 5; Worcester et al., 1993; Pawlowicz et al., 1995; Morawitz et al., 1996; Sutton et al., 1997). As part of an on-going experiment in the Labrador Sea, heat content is being measured acoustically (Fig. 6; Send and Kindler, 2001).

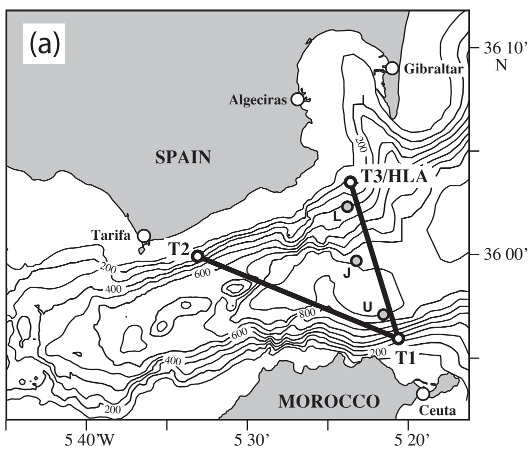

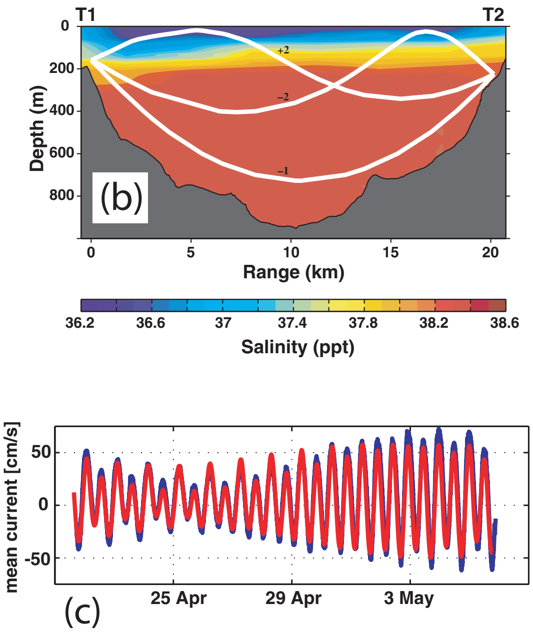

Fig. 4 (a) Location of acoustic instruments at the eastern entrance of the Strait of Gibraltar. (b) Horizontal and depth sampling by ray paths along path T1-T2. (c) A two-week comparison of along-strait current averaged along a deep-turning ray across the Strait (black) and the tidal and low-frequency flow field determined from a wide range of direct current observations (red).

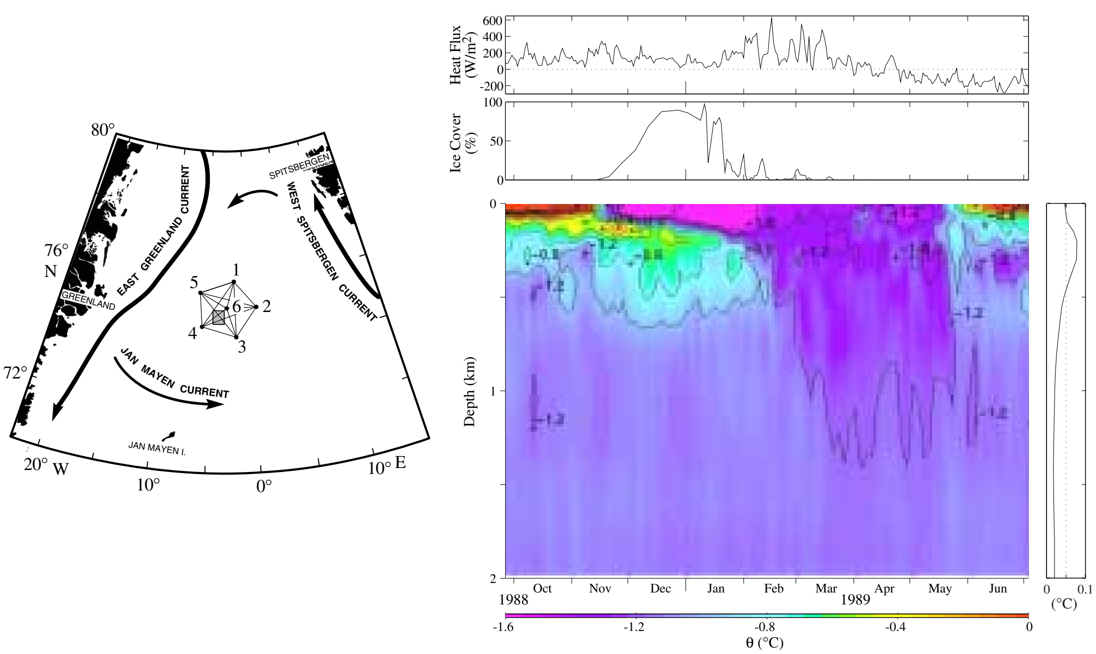

Fig. 5. (Left) Geometry of the tomography array in the Greenland Sea during 1988–1989. A deep convective chimney was observed near the center of the array during March 1989 (shaded region). (Right) Time-depth evolution of potential temperature averaged over the chimney region. Typical rms uncertainty as a function of depth is shown to the right. Total surface heat flux and daily averaged ice cover are shown above. Convection occurs in March, with cold water extending from the surface to depth. It occurs when the area becomes ice-free and large amounts of heat are lost to the cold atmosphere.

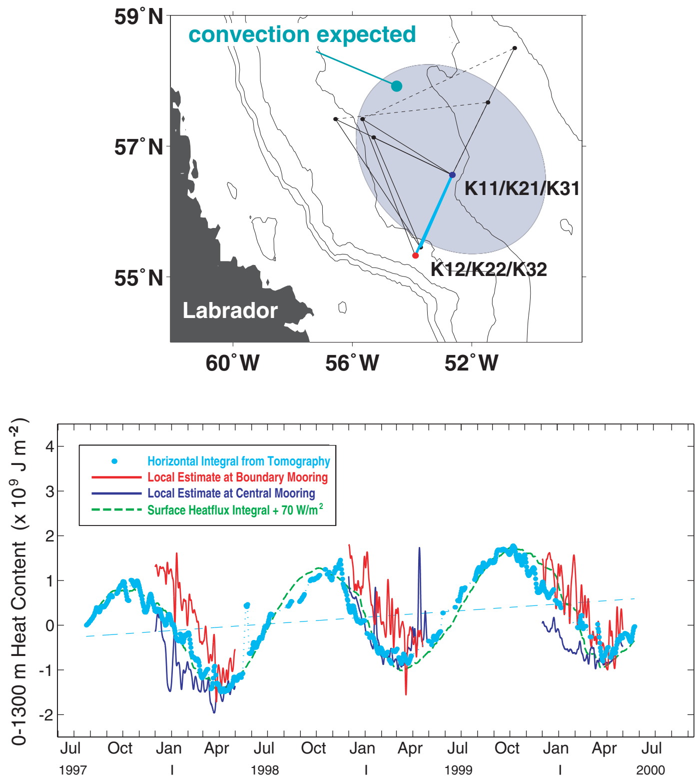

Fig. 6. (Top) In the Labrador Sea, the tomography mooring arrays were deployed in different years in the area where deep convection activity is expected (shaded). (Bottom) A three-year time series of 0–1300-m heat content derived from tomographic data (cyan, dots) along the section marked in the top panel and derived from data obtained at the moorings at the ends of the section (blue: K11, red: K12). The dashed line shows a three-year warming trend, equivalent to a heat flux of 10 Wm^{-2}. The dashed green curve is the time-integral of the NCEP surface heat fluxes, corrected by the addition of 70 Wm^{-2}, averaged over the section.

3. BASIN SCALES

3.1 *ACOUS–Arctic Climate Observations Using Underwater Sound*

The Arctic is ideally suited to measurement by acoustic tomography. It has low acoustic noise levels and no internal waves so the acoustic propagation is very clean. Travel times of the first several acoustic modes are resolved readily, and these modes naturally sample the layers in the water column that are of oceanographic interest. Finally, it is difficult to access the arctic water column by conventional techniques; acoustics provide perhaps the only way to remotely sense the sub-surface variability (Mikhalevsky et al., 1995, 1999).

In the 1994 Trans-Arctic Acoustic Propagation (TAP) experiment, transmissions were made from a site north of the Svalbard Archipelago across the entire Arctic Ocean to receiving arrays located in the Lincoln and the Beaufort seas (Fig. 7). Whether the results shown here are due to global climate warming or a natural oscillation is an area of active research.

A future notional monitoring grid in the Arctic Ocean to exploit synoptic acoustic remote sensing with *in situ* measurements is shown in Fig. 8.

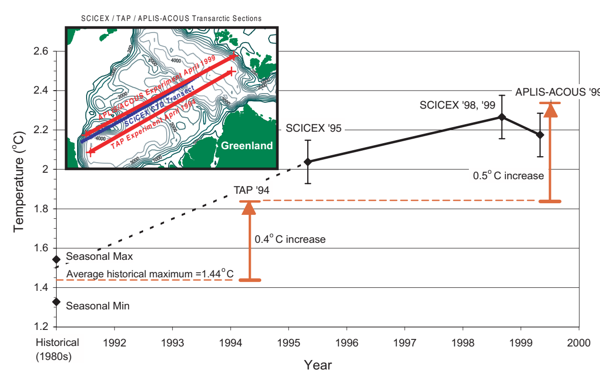

Fig. 7. Temperature of the Atlantic Layer obtained from historical climatology and from the (submarine) SCICEX 1995, 1998, and 1999 transects. The SCICEX transects were close to the 1994 TAP and 1999 ACOUS/APLIS propagation paths. The red arrows indicated the change in the maximum temperature inferred from the acoustic travel time changes.

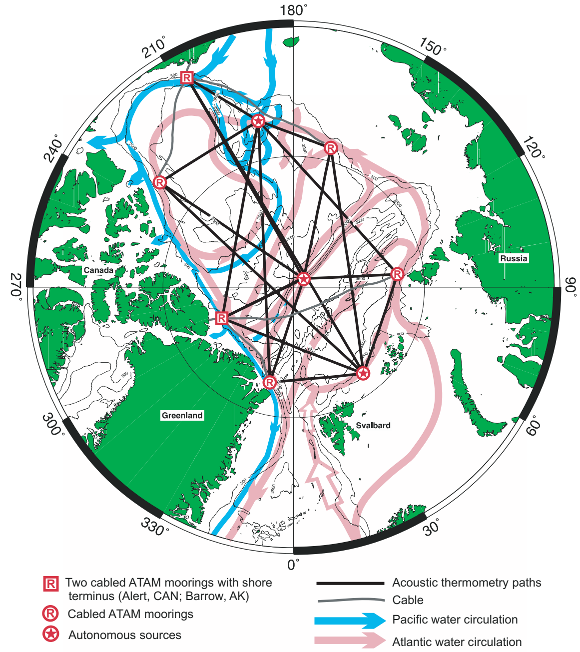

Fig. 8. A future notional monitoring grid in the Arctic Ocean with instruments cabled to shore at Alert, Canada, and Barrow, Alaska. ATAM stands for Acoustic Thermometry and Autonomous Monitoring.

3.2 *ATOC–Acoustic Thermometry of Ocean Climate*

The goal of the ATOC project is to measure the ocean temperature on basin scales and to understand the variability. The acoustic measurements inherently average out mesoscale and internal wave noise that contaminate point measurements (The ATOC Consortium, 1998; Dushaw et al., 1999; Worcester et al., 1999). The ATOC acoustic paths in the Pacific are shown in Fig. 9.

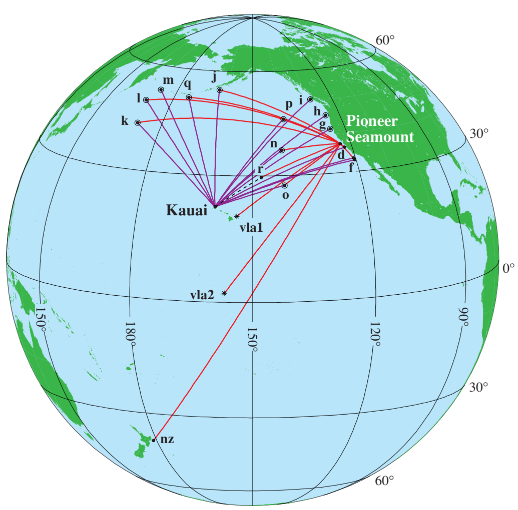

Fig. 9. ATOC acoustic paths in the North Pacific. The letters k, l, etc., are arbitrary names of receivers such as the U.S. Navy SOSUS arrays.

Depth-averaged ATOC temperature measurements are compared with historical data and temperature derived from satellite altimetry data (Fig. 10). The acoustic data are smooth and exhibit small error bars, especially for the long (5 Mm) paths.

The travel time data from all the various acoustic paths can be used to reconstruct the depth-averaged horizontal sound speed (temperature) field (Fig. 11). This map gives an indication of the scales that can be resolved. This map can be made every few days or so, and when spatially averaged, can yield average ocean temperature with high accuracy.

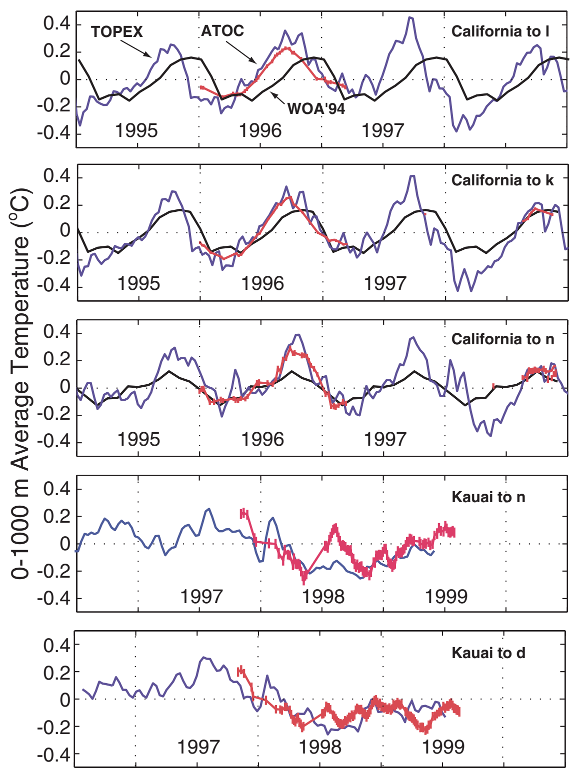

Fig. 10. The 0–1000-m depth-averaged ATOC temperature measurements (red, with error bars) are compared with historical data (WOA '94) and the temperature derived from TOPEX/POSEIDON (T/P) altimetry (blue, assuming sea surface height variations are caused only by thermal expansion). The means have been removed from all time series. In the lower two panels, the annual cycle has been removed from the T/P data; the acoustic rays on these particular paths sample below the seasonally varying surface layers, so they do not observe the annual cycle.

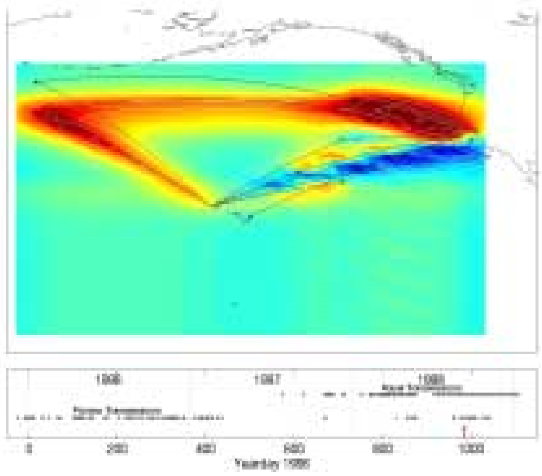

Fig. 11. Depth-averaged horizontal sound speed (temperature ±0.125°C, 0–1000-m depth average) field reconstructed from all the travel time data.

To obtain a feeling for the power of the spatial integration associated with the acoustic data, depth-averaged temperature from the Hawaii Ocean Time-series (HOT) is plotted with satellite altimetry data (Fig. 12). The point measurements have large fluctuations in temperature caused by mesoscale variability. The differences between the temperature inferred from T/P and the direct measurement at HOT are comparable to the temperature signal observed in the line-integrating data.

4. THE FUTURE

Ocean acoustic tomography will continue to be used to study ocean processes that can only be addressed using the unique sampling of the method (e.g., integral heat content and current velocity) or remote sensing capability (e.g., the Arctic and Strait of Gibraltar). Regional experiments have been conducted recently and are continuing in the North Pacific (Fig. 13). The present ATOC basin scale array will continue to be expanded (Fig. 14), and new arrays are in the planning process for the Atlantic (Fig. 15) and the Indian oceans (http://deos.rsmas.miami.edu/; SCOR WG 96, 1994; Barton et al., 2000).

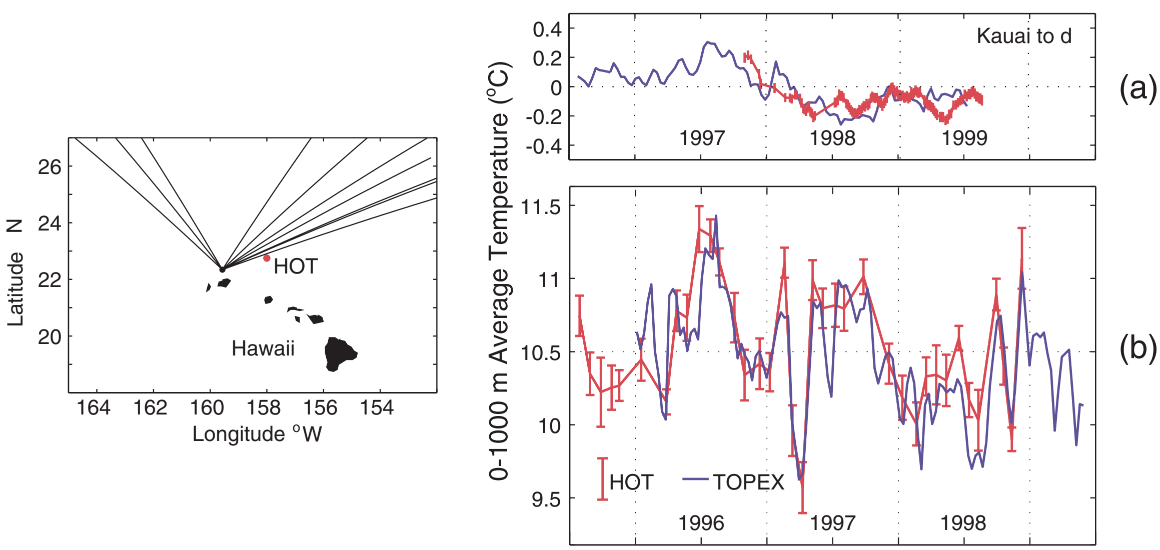

Fig. 12. Data from the Hawaii Ocean Time-series (HOT) site (about 100 km north of Oahu) are plotted with TOPEX altimetry data. The 0–1000-m averaged temperature is plotted on the same scale as above. The HOT data points show the average and rms of 10–20 CTD casts obtained during each HOT cruise.

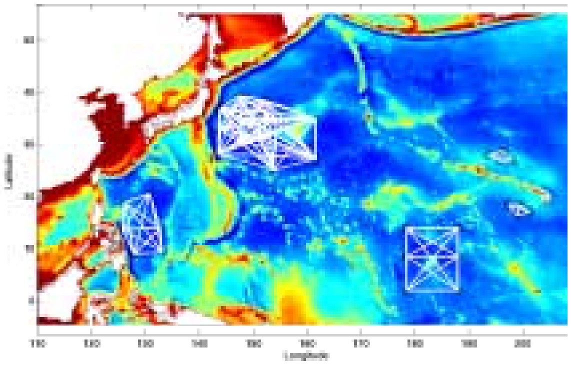

Fig. 13. Regional acoustic tomography arrays in the North Pacific: The Central Equatorial Pacific Tomography Experiment (CEPTE) just north of the equator has recently finished. The Hawaiian Ocean Mixing Experiment (HOME) tomography arrays were deployed in 2001. The Kuroshio Extension System Study (KESS) tomography array may be deployed in the next few years. The North Equatorial Current Bifurcation Region Experiment in the Philippine Sea may begin in 2006.

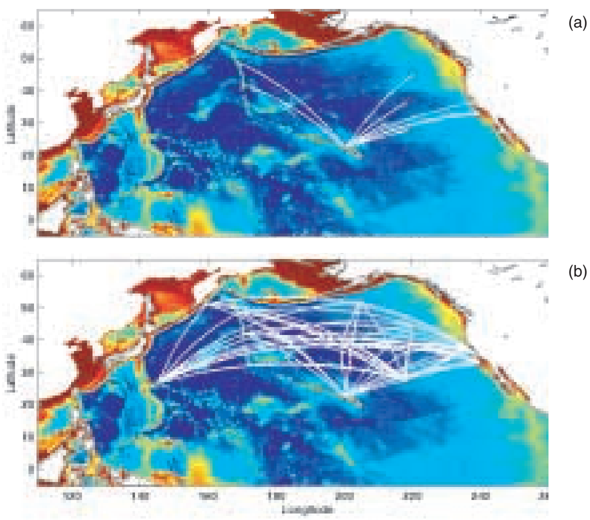

Fig. 14. (a) Acoustic data will be obtained on this minimal acoustic array for the next five years. The Kauai ATOC source and U.S. Navy SOSUS receivers are used. (b) Fairly dense acoustic sampling of the North Pacific can be obtained with the addition of acoustic sources: a replacement source off the coast of California, a source near Japan, an "H2O" acoustic source midway between Hawaii and California, and an acoustic source that might be attached to a DEOS mooring in the central North Pacific.

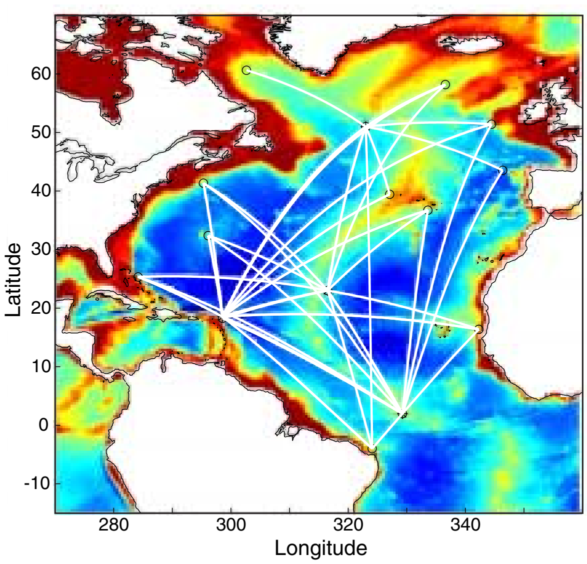

Fig. 15. A notional array for the North Atlantic consists of 4 cabled-to-shore or autonomous acoustic sources, together with about 10 receivers at SOSUS sites and on DEOS moorings. Simple receivers mounted on moorings-of-opportunity can further increase the acoustic sampling at little additional cost. Tomographic instruments deployed by European organizations in the North Atlantic in the coming decade will contribute to this array. Such a network would complement existing observation systems for ocean climate variability.

Acknowledgements This paper is based on that by Dushaw et al., 2001, that had its origins in the "OceanObs99" meeting in San Rafael, France, in 1999.

The posters associated with this work can be found at http://staff.washington.edu/dushaw.

REFERENCES

The Acoustic Mid-Ocean Dynamics Experiment (AMODE) Group, 1994: Moving ship tomography in the North Atlantic, *EOS Trans. AGU*, **75**, 17, 21, and 23.

The ATOC Consortium, 1998: Ocean climate change: Comparison of acoustic tomography, satellite altimetry, and modeling, *Science*, **281**, 1327–1332.

Cornuelle, B. D., W. H. Munk, and P. F. Worcester, 1989: Ocean acoustic tomography from ships, *J. Geophys. Res.*, **94**, 6232–6250.

Dushaw, B. D., P. F. Worcester, B. D. Cornuelle, and B. M. Howe, 1993: Variability of heat content in the Central North Pacific in summer 1987 determined from long-range acoustic transmissions, *J. Phys. Oceanogr.*, **23,** 2650–2666.

Dushaw, B., G. Bold, C.-S. Chiu, J. Colosi, B. Cornuelle, Y. Desaubies, M. Dzieciuch, A. Forbes, F. Gaillard, A. Gavrilov, J. Gould, B. Howe, M. Lawrence, J. Lynch, D. Menemenlis, J. Mercer, P. Mikhalevsky, W. Munk, I. Nakano, F. Schott, U. Send, R. Spindel, T. Terre, P. Worcester, C. Wunsch, 2001: Observing the Ocean in the 2000's: A Strategy for the Role of Acoustic Tomography in Ocean Climate Observation. In: *Observing the Ocean in the 21st Century*, C.J. Koblinsky and N.R. Smith (eds), Bureau of Meteorology, Melbourne, Australia, in press.

Dushaw, B. D., P. F. Worcester, B. D. Cornuelle, and B. M. Howe, 1994: Barotropic currents and relative vorticity in the central North Pacific during summer 1987 determined from long-range reciprocal acoustic transmissions, *J. Geophys. Res.*, **99**, 3263–3272.

Dushaw, B. D., 1999: Inversion of multimegameter-range acoustic data for ocean temperature, *IEEE J. Ocean. Eng.*, **24**, 215–223.

Mikhalevsky, P. N., A. B. Baggeroer, A. N. Gavrilov, and M. Slavinsky, 1995: Experiment tests use of acoustics to monitor temperature and ice in the Arctic Ocean, *EOS, Trans. AGU*, **76**, 27.

Mikhalevsky, P. N., A. Gavrilov, and A. B. Baggeroer, 1999: The transarctic acoustic propagation experiment and climate monitoring in the Arctic, *IEEE J. Ocean. Eng.*, **24**, 183–201.

Morawitz, W. M. L., P. J. Sutton, P. F. Worcester, B. D. Cornuelle, J. F. Lynch, and R. Pawlowicz, 1996: Three-dimensional observations of a deep convective chimney in the Greenland Sea during winter 1988/1989, *J. Phys. Oceanogr.*, **26**, 2316–2343.

Munk, W., and C. Wunsch, 1979: Ocean acoustic tomography: A scheme for large scale monitoring, *Deep-Sea Res.*, **26**, 123–161.

Munk, W., and C. Wunsch, 1982: Observing the ocean in the 1990s, *Phil. Trans. R. Soc. A,* **307**, 439–64.

Munk, W., P. Worcester, and C. Wunsch, 1995: *Ocean Acoustic Tomography,* Cambridge University Press, Cambridge.

Pawlowicz, R., J. F. Lynch, W. B. Owens, P. F. Worcester, and W. M. L. Morawitz, 1995: Thermal evolution of the Greenland Sea Gyre in 1988–89, *J. Geophys. Res.*, **100**, 4727–4750.

SCOR WG 96 (Scientific Committee on Ocean Research Working Group 96; Atlantic sub-group: W. J. Gould, Y. Desaubies, B. M. Howe, D. R. Palmer, F. Schott, and C. Wunsch), 1994: Acoustic Thermometry in the Atlantic: A Report to SCOR WG 96.

Send, U., P. F. Worcester, B. D. Cornuelle, C. O. Tiemann, and B. Baschek, 2000: Integral measurements of mass transport and heat content in straits from acoustic transmissions, *Deep-Sea Res.*, submitted.

Sutton, P. J., W. M. L. Morawitz, P. F. Worcester, and B. D. Cornuelle, 1997: Temperature evolution of the upper ocean in the Greenland Sea January to March 1989, *J. Geophys. Res.*, **102**, 27,861–27,874.

Worcester, P. F., J. F. Lynch, W. M. Morawitz, R. Pawlowicz, P. J. Sutton, B. D. Cornuelle, O. M. Johannessen, W. H. Munk, W. B. Owens, R. Shuchman, and R. C. Spindel, 1993: Ocean acoustic tomography in the Greenland Sea, *Geophys. Res. Lett.*, **20**, 2211–2212.

Worcester, P. F., B. D. Cornuelle, M. A. Dzieciuch, W. H. Munk, B. M. Howe, J. A. Mercer, R. C. Spindel, J. A. Colosi, K. Metzger, T. G. Birdsall, and A. B. Baggeroer, 1999: A test of basin-scale acoustic thermometry using a large-aperture vertical array at 3250-km range in the eastern North Pacific Ocean, *J. Acoust. Soc. Am.*, **105**, 3185–3201.